# New antenna diversity front-end using code multiplexing

Matthieu Gautier[1,2], Ioan Burciu[1,2] and Guillaume Villemaud[1]
[1]Université de Lyon, INRIA, INSA-Lyon, CITI - F-69621 - France
firstmane.lastname@insa-lyon.fr
[2]Orange Labs - 28, chemin du vieux chêne - 38243 Meylan - France

***Abstract*— In this paper, we address the architecture of an antenna diversity receiver. An innovative architecture has been introduced based on code multiplexing, it significantly reduces the power consumption of the front-end. This architecture uses the direct sequence spread spectrum technique in order to multiplex the different antennas contributions through a single IQ demodulator. This paper address the performances of this kind of architecture. Simulation and measurement results show that, in a Gaussian case, the bit error rate does not increase significantly with the multiplexing. IQ imbalance study shows that the new architecture has the same sensitivity to IQ mismatches than the classical stack-up architecture.**

## I. Introduction

Introduced in 1984 by J.H. Winters [1], the antenna diversity techniques are an interesting solution for future communication systems. They are used to increase the capacity and performances (quality of service QoS, datarate, ... ) of wireless networks. Most studies on antenna diversity systems concern the digital algorithms [2][3] (beamforming, space-time coding, spatial multiplexing, ... ) and the types of antenna arrays [4] such as spatial diversity, pattern diversity, polarization diversity, ...

But the analog complexity issue concerning an antenna diversity receiver using digital antenna processing has been very little addressed [5]. In fact, the performance gain achieved by the diversity implies an increase of the digital complexity (algorithms implementation), but also an increase of the complexity and the consumption of the analog front-end because each additional antenna induces a complete additional analog branch [6].

Therefore this paper deals with the architecture of the analog front-end associated with these techniques. We explores the use of a single common front-end for the processing of signals received by the antennas. The use of one common analog chain underlies the idea of multiplexing the different branches on a single front-end. Introduced by authors in an international patent [7], we propose a novel architecture that uses orthogonal codes in order to multiplex the different antennas contributions through a single IQ demodulator. It has been shown that this architecture significantly reduces the complexity of the analog front-end [8].

This paper ensures the functionality of such a receiver: Bit Error Rate (BER) simulations have been performed, the IQ imbalance sensitivity [9] is studied and more realistic results have been measured by using an Agilent Technologies connected solution as presented in [10].

This paper consists of 4 parts. Following this introduction, Sec. II presents the new antenna diversity front-end by giving implementation and theoretical aspects. Sec. III details some simulated and measured performances including the IQ imbalance sensitivity. Finally, conclusions are drawn and follow-ups are provided.

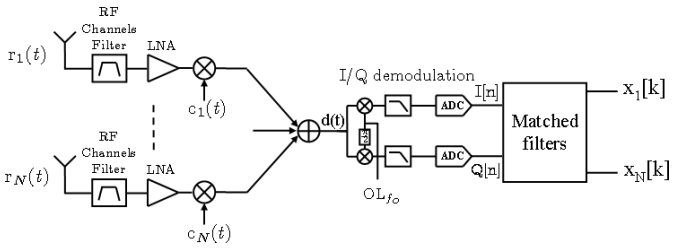


Fig. 1. Analog and digital front-end of the code multiplexing architecture.

## II. The code multiplexing architecture

### A. Implementations aspects

In order to have a performance improvement, a transceiver using antenna diversity [1] has to use several antennas for its transmitter and/or receiver. The classical analog front-end of such a receiver is based on the RF stack-up architecture [5]. It uses one dedicated analog chain for each of the $N$ antennas. Each of theses chains transforms the radiofrequency (RF) signal $\{r_k(t), k{=}1, \ldots, N\}$ in baseband signals in-phase $I_k(t)$ and in-quadrature $Q_k(t)$ [11]. This RF stack-up architecture is an obvious choice: having $N$ separated dedicated chains allows the demodulation of each branch with a significant quality (high Signal to Noise Ratio - SNR at the ADC input). However, this choice enforces a high complexity of the analog front-end. The proposed architecture aims to reduce this complexity without decreasing the SNR quality after branches demodulation.

In [8], we show that the code domain appears to be the most suited for an antenna diversity receiver, compared to temporal and frequency domains. In order to achieve the spectrum overlapping, decorrelation can be done by the spread spectrum technique. The direct sequence spread spectrum (DSSS) technique is the basis of code division multiple access (CDMA) technology [12]. The spread spectrum allows a multiplexing which is neither time nor frequency, but a code multiplexing. The theoretical aspects of the proposed structure are described in the next part.

The novel antenna diversity receiver using code multiplexing is depicted in Fig. 1 and consists in 2 parts: the analog

multiplexing and the digital demultiplexing.

*Analog coding:* After one dedicated antenna, each chain is composed of an SAW RF filter (Surface Acoustic Wave filter) for the band selection and a LNA (Low Noise Amplifier). The DSSS consists in allocating a spreading code to each branch, all these codes being orthogonal two by two. Each received signal that carries information is multiplied by the code $c_k(t)$ which is a pseudo-random sequence of $N$ binary entities having a rate $N$ times higher than the symbol. Then, an adding operation between the spread contributions is done and the signal is transposed to the baseband domain by an IQ demodulator that recovers the in-phase and in-quadrature signals. The $I(t)$ and $Q(t)$ signals are then digitized by two analog to digital converters (ADC).

*Digital decoding*: So far, the different steps will be implemented in the analog part of the receiver. The decoding step will be performed digitally. It consists in applying digital matched filters.

The proposed architecture works for any multi-antenna schemes: for every antenna array and every digital algorithm. However, a limitation of the concept of using orthogonal spreading codes is that only an even number (2, 4, 8,...) of antennas can be received. The synchronization between coding and decoding is not such an important issue as during an UMTS transmission. Indeed, the propagation delay of the spread signal through the circuit path is well-predicted through accurate circuit analysis and simulation. Therefore, attaining synchronization between the spreading and despreading codes is a trivial matter. For this reason, time delay between the spreading and despreading codes is neglected in this study.

To illustrate the code multiplexing, Fig. 2 shows the power spectrum of the signal before and after code multiplexing. We use a $N$=4 antennas system that receives an IEEE 802.11g [13] type signal having a 20 MHz bandwidth and a 2412 MHz RF frequency. The codes have a rate $N$ times higher than the symbol, so the resulting signal has variations that are $N$ times faster than the information signal, increasing $N$ times the bandwidth of the signal frequency spectrum. Fig. 2 shows that the frequency bandwidth after coding is 80 MHz. Indeed, the multiplex operation generates a $N$=4 bandwidth increase factor.

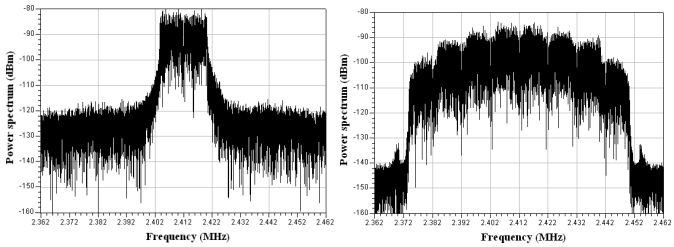


Fig. 2. Power spectral density before and after code multiplexing.

### B. System model of code multiplexing receiver

In this section, we give the theoretical aspects of the application of the direct sequence spread spectrum to an antenna diversity receiver.

*Analog coding:* First, let us look at the $k^{th}$ antenna contribution. The digital transmitted message is made of complex symbols $x_k[i]$ which depend on the digital modulation (QAM, OFDM, ...). These symbols are transmitted at the symbol rate $D_s = 1/T_s$ where $T_s$ is the symbol duration. The digital baseband signal (analog signal carrying digital information), with a rectangular pulse shaping, is written:

$$x_k(t) = \sum_{i=-\infty}^{+\infty} x_k[i] p_{T_s}(t - iT_s) \text{ with } p_{T_s} = \begin{cases} 1 \text{ if } 0 \leq t < T_s, \\ 0 \text{ else.} \end{cases} \quad (1)$$

The RF transmitted signal is real and is defined by:

$$s_k(t) = x_k(t) e^{j2\pi f_0 t} + x_k^*(t) e^{-j2\pi f_0 t}, \quad (2)$$

with $f_0$ the RF modulating frequency.
In an ideal transmission through a non-dispersive channel, the received signal is expressed by:

$$r_k(t) = A_k s_k(t) + n_k^{RF}(t), \quad (3)$$

with $A_k$ the path loss attenuation and $n_k^{RF}(t)$ the total RF noise at the input of the $k^{th}$ antenna.
In order to perform the code multiplexing of all the branches, each received signal is spread using a code $c_k(t), k = 1, \dots N$. The pseudo-random sequences are $T_s$-periodic. By using a limited symbol duration code, repeated indefinitely, the system has an easier sequence generation as well as a better despreading synchronization. For a given branch $k$, a set of $N$ binary (complex binary) chips $\{c_k[n],\ n = 0, \dots N-1\}$ is used. This sequence is called "spreading code". The periodic code $c_k^{per}(t)$ is the periodic pseudo-random sequence:

$$c_k^{per}(t) = \sum_{i=-\infty}^{+\infty} \sum_{n=0}^{N-1} c_k[n] p_{T_c}(t - nT_c) p_{T_s}(t - iT_s), \quad (4)$$

where $T_c$ is the chip duration and $N = \frac{T_s}{T_c}$ is the code length. The use of codes with a $N$ length allows the reception of $N$ antennas.
The $k^{th}$ antenna contribution after spreading $d_k(t)$ is expressed by:

$$d_k(t) = A_k c_k^{per}(t) s_k(t) + c_k^{per}(t) n_k^{RF}(t). \quad (5)$$

By replacing $s_k(t)$ by (2), we get:

$$d_k(t) = A_k c_k^{per}(t) \{x_k(t) e^{j2\pi f_0 t} + x_k^*(t) e^{-j2\pi f_0 t}\} + c_k^{per}(t) n_k^{RF}(t). \quad (6)$$

Once the coding operation ended for each antenna, the new signals intercorrelations depend only on the codes intercorrelations. So, signals can be clearly overlapped in time and frequency, as they are separable by their spreading sequence. The adding operation between the spread contributions can be done:

$$d(t) = \sum_{k=1}^{N} d_k(t). \quad (7)$$

The spread spectrum of $d(t)$ can be seen in Fig. 2.

After the code multiplexing step, the signal $d(t)$ is transposed to the baseband frequency by an IQ demodulator. $I(t)$ is the in-phase component and $Q(t)$ is the in-quadrature component. $LP[\bullet]$ refers to an ideal low-pass filter having a bandwidth of $B_d/2$ ($B_d$ is bandwidth of $d(t)$). $I(t)$ and $Q(t)$ are expressed by:

$$I(t) = LP[d(t)\cos(2\pi f_0 t)] \tag{8}$$

$$= \sum_{k=1}^{N} \{\frac{A_k}{2} c_k^{per}(t)(x_k(t) + x_k^*(t)) + c_k^{per}(t) n_k^{RF}(t)\cos(2\pi f_0 t)\}, \tag{9}$$

$$Q(t) = LP[d(t)\sin(2\pi f_0 t)] \tag{10}$$

$$= \sum_{k=1}^{N} \{A_k \frac{j}{2} c_k^{per}(t)(x_k^*(t) - x_k(t)) + c_k^{per}(t) n_k^{RF}(t)\sin(2\pi f_0 t)\}. \tag{11}$$

After demodulation, the signal is defined by its complex envelope:

$$\hat{x}(t) = I(t) + jQ(t) = \sum_{k=1}^{N} \{c_k^{per}(t) x_k(t) + c_k^{per}(t) n_k^{BB}(t)\}, \tag{12}$$

where $n_k^{RF}(t) = Re\left[n_k^{BB}(t) e^{j2\pi f_0 t}\right]$.

*Digital decoding*: The pseudo-random sequence modulating the symbols during the spreading step has to be known by the decoder in order to enable the reconstruction of symbols by successive correlations (despreading and integration on the symbol time) between the spreading signal and the same coding sequence:

$$\hat{x}_l[m] = \frac{1}{T_s} \int_{mT_s}^{(m+1)T_s} \hat{x}(t) c_l^*(t) dt, \quad mT_s \leq t < (m+1)T_s, \tag{13}$$

$$= \frac{1}{T_s} \sum_{k=1}^{N} \{A_k x_k[m] + n_k^{BB}(t)\} \int_0^{T_s} c_k(t) c_l^*(t) dt. \tag{14}$$

Intercorrelation properties of the code influence the performances (detection and synchronization) of a spread spectrum system that operates by correlation between signals and codes. If the codes are orthogonals, their intercorrelation functions are defined by:

$$\frac{1}{T_s} \int_0^{T_s} c_k(t-\tau) c_l^*(t) dt = \delta[k-l]. \tag{15}$$

As a final result, we get:

$$\hat{x}_l[m] = \sum_{k=1}^{N} \{A_k x_k[m] + n_k^{BB}(t)\} \delta[k-l], \tag{16}$$

$$= A_l x_l[m] + n_l^{BB}(t). \tag{17}$$

The digital baseband symbols $\{x_l[m],\ l = 1 \ldots K,\ m \in \mathbb{Z}\}$ received on each antenna are recovered.

## III. Simulated and experimental validation

The functionality of such a receiver is validated in this part by using several BER simulations and measurements. First, two complete IEEE 802.11g [13] transmission systems have been modeled using the Advanced Design System (ADS) software [14]: one using the classical stack-up homodyne front-end, the other using the code multiplexing front-end. Then a connected solution [10] has been realized for both solutions in order to obtain realistic measurements.

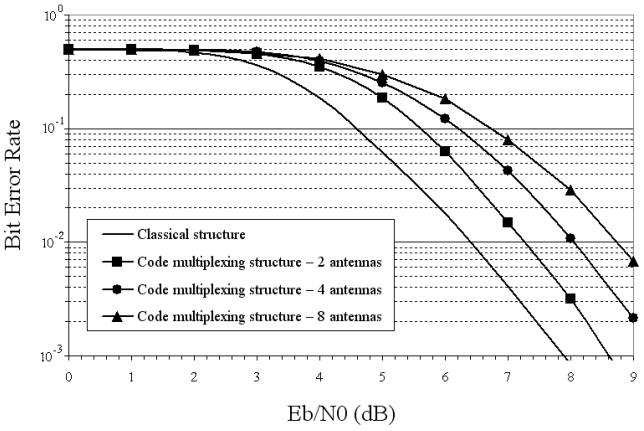


Fig. 3. BER versus $\frac{E_b}{N_0}$ for different number of antennas.

### A. System description

The implemented system is described in Fig 1. Each antenna receives an IEEE 802.11g type signal. The channel bandwidth is 20 MHz, the RF frequency is 2412 MHz and the datarate is 6 Mbit/s. The signals $r_k(t)$ are multiplied by the periodical spreading codes $c_k(t)$. The sum of $N$ encoded signals is then performed in order to generate the radio-frequency multiplex signal $d(t)$. This signal is then transformed by an IQ demodulator. After the sampling step, we apply matched filters consisting in a digital filter (impulse response $c_k^*[n]$) followed by a subsampling operation.
We suppose that the received signal provided by an antenna is independent of those received from the other antennas. We also consider a perfect code synchronization. We choose Walsh-Hadamard codes [15] as those used by the UMTS standard. The signal $r_1(t)$ from the first antenna is not spread because its associated code $c_1(t)$ is only composed of '1'. Thus, the performances are given only for the second antenna which is coded by a non-unitary code $c_2(t)$.

### B. Simulations results

*1) BER performances:* Simulated performances of the code multiplexing architecture for an Additive White Gaussian Noise (AWGN) channel are compared to the performances of a classical homodyne structure. The BER evolutions as a function of $\frac{E_b}{N_0}$ are shown in Fig. 3. The figure shows the influence of the number of multiplexed antennas on the BER evolution. A $N$=2, $N$=4 and $N$=8 antennas receiver are tested. We consider only the transmission quality of the second antenna, but the results are equal for each the antenna.
Simulations results show that, in an ideal no imperfections case (no multipath channel, no RF impairments), the structure using code multiplexing decreases the performances by

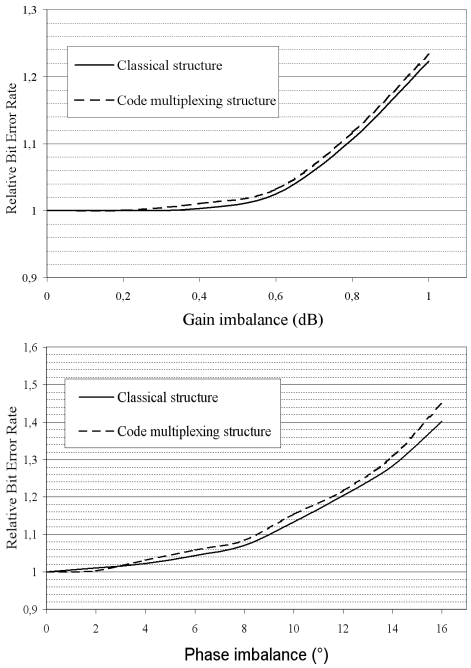


Fig. 4. Relative BER versus gain imbalance and versus phase imbalance.

less than 1 dB at a $BER = 10^{-2}$ for a $N$=2 antennas receiver. The $\frac{E_b}{N_0}$ degradation increases with the number of antennas, it reaches 2.3 dB for a $N$=8 antennas system. This degradation is due to digital aliasing during the subsampling step after filtering. Future work is to reduce this aliasing effect.

*2) IQ imbalance sensibility:* This RF impairement means that there is a loss of orthogonality between the I and Q branches, which is due to a gain mismatch $g$ and a phase mismatch $\varphi$ between the two local oscillators [9]. The phase mismatch is caused by a non-ideal layout which means that the lines between mixers are not strictly equal. The gain mismatch is due to a difference of the conversion gain between the I and Q mixers. By taking into account IQ imbalance, Eq. (8) and Eq. (10) become:

$$I(t) = LP[d(t)\cos(2\pi f_0 t)], \tag{18}$$

$$Q(t) = LP[d(t)g\sin(2\pi f_0 t + \varphi)]. \tag{19}$$

As a final result, Eq. (17) becomes:

$$\hat{x}_l[m] = \frac{A_l}{2}\{x_l[m](1+ge^{j\varphi})+x_l^*[m](1-ge^{-j\varphi})\}+n_l^{BB}(t). \tag{20}$$

The IQ imbalance results depicted in (20) is the same as a classical IQ receiver [9].

Fig. 4 gives the simulated normalized BER evolution as a function of the gain and the phase imbalance. The power level conditions leads to a $10^{-3}$ level of BER under ideal IQ mismatch conditions. Simulated performances of the code multiplexing architecture are compared to the performances of a classical homodyne structure. Simulations have been done in the same conditions described in the previous paragraph for a $N$=4 antennas system.

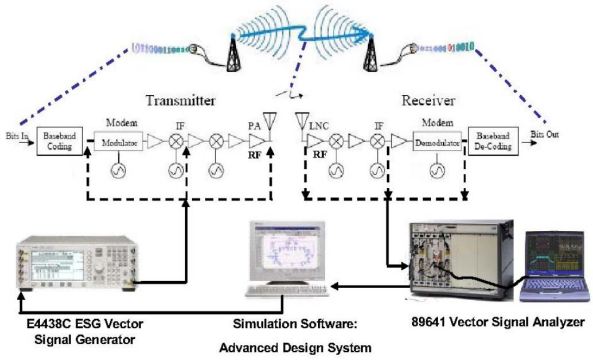


Fig. 5. The platform structure for a 1x1 transmission.

According to theory, simulation results show that the new code multiplexing architecture has nearly the same sensibility as the classical homodyne architecture.

### C. Experimental results

For the experimental validation [10], we use a radio platform described in Fig. 5. This platform is made of high technology equipments developed by Agilent Technologies [14]: the ADS software and measurement hardware which are two arbitrary waveform generators (ESG 4438C) and a vector spectrum analyzer (VSA89641) having two RF inputs. The arbitrary waveform generator is able to generate any complex signal which is then possible to analyze after propagation with the vector spectrum analyzer. The vectorial analysis software can demodulate this signal in order to accurately estimate the transmission system quality.

With this connected solution, a software/hardware interaction allows us to test and conceive very complex and realistic systems. We can therefore estimate the impact of the different imperfections of the RF front-end (phase noise, distortion, IQ imbalance, ...) and also the impact of the propagation environment (AWGN , multipath, fading, ...). Using the two RF inputs of the VSA allows us to analyze and evaluate the performance of an antenna diversity system using two antennas. So, the experimental measurements are performed for both the classical and the code multiplexing architectures using $N$=2 antennas.

BER measurements are realized for an AWGN channel and for different SNR of the antennas inputs. The measures are given for both the code multiplexing architecture and the classical homodyne structure and are compared with the performances obtained by simulation in Fig 3. The BER evolutions of the second antenna are shown in Fig. 6.

Compared to the simulated results, the measured results are somewhat degraded, the difference is due to the channel used for the measurement which may not exactly be an AWGN one. The $\frac{E_b}{N_0}$ gap between the classical and code multiplexing structures is almost the same during the measurements as that obtained during the simulations. It turns around 1 dB for a $BER = 10^{-2}$.

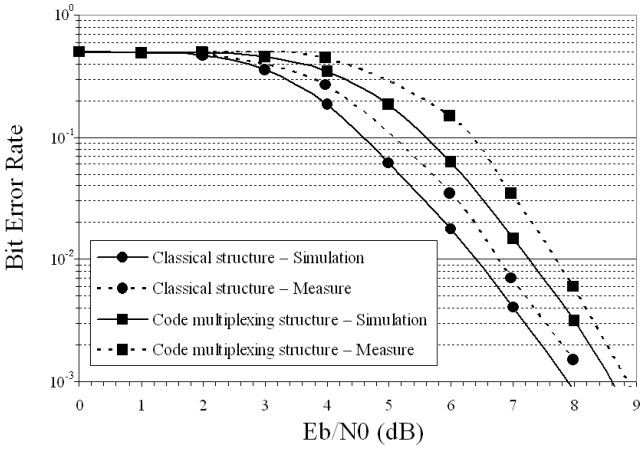


Fig. 6. Simulated and measured BER versus $\frac{E_b}{N_0}$ for a 2 antennas receiver.

## IV. Conclusions

In this paper, we present a novel architecture for an antenna diversity receiver. The proposed structure uses orthogonal codes to multiplex the different branches through a single IQ demodulator. The main goal was to reduce the complexity of the analog front-end. The system reduces the number of ADC by using only two ADC instead of the $2N$ used by the classic receiver. Meanwhile, specifications of the ADC in terms of bandwidth are much more stringent. [8] shows that a power consumption reduction of 20% could be reached for a $N = 8$ antennas system.

The points revealed in this study are the evaluation of the feasibility of such a structure. The implementation of analog coding and digital decoding has been validated by BER simulations and measurements. Results show that, in a Gaussian case, the bit error rate does not increase so much with the multiplexing.

IQ imbalance study shows that the new architecture has the same sensitivity to IQ mismatches than the classical architecture. We note that the resulting IQ influence is the same for each baseband contribution whereas the IQ influence depends on each dedicated IQ demodulator for a classical structure.

The follow-ups of this work are to accurately define the specifications of the analog components. An extension to multi-channel receiver has to be studied as well as its resulting complexity-performance trade-off.

A patent is pending on the proposed architecture [7].

## Acknowledgment

The authors would like to thank Orange Labs which supporte this study.

## References

[1] J.H. Winters, "Optimum Combining in Digital Mobile Radio with Cochannel Interference," *IEEE Journal on Selected Areas in Communications*, vol. 2, no. 4, pp. 528–539, July 1984.

[2] S.M. Alamouti, "A Simple Transmit Diversity Technique for Wireless Communications," *IEEE Journal on Selected Areas in Communications*, vol. 16, no. 8, pp. 1451–1458, October 1998.

[3] I. E. Telatar, "Capacity of Multi-Antenna Gaussian Channels," *AT&T Bell Labs., Murray Hill, NJ, Intern. Tech. Memo*, June 1995.

[4] C.B. Dietrich, K. Dietze, J.R. Nealy, and W.L. Stutzman, "Spatial, Polarization and Pattern Diversity for Wireless Handheld Terminals," *IEEE Transactions on Antennas and Propagation*, vol. 49, no. 9, pp. 1271–1281, September 2001.

[5] T. Kaiser, A. Bourdoux, H. Boche, J. Rodriguez Fonollosa, J. Bach Andersen, and W. Utschick, *Smart Antennas: State of the Art*, Eurasip Book Series on Signal Processing & Communications, 2005.

[6] H. Tsurumi and Y. Suzuki, "Broadband RF stage architecture for software-defined radio inhandheld terminal applications," *IEEE Communications Magazine*, vol. 37, no. 2, pp. 90–95, February 1999.

[7] M. Gautier and G. Villemaud, *Diversity receiver: analog complexity reduction by using mutiplexing technique*, International patent pending (INPI number: 0759667), applicant: Orange Lab, December 2007.

[8] M. Gautier and G. Villemaud, "Low complexity antenna diversity front-end: Use of code multiplexing," *Proceedings of IEEE Wireless Communication and Networking Conference (WCNC09)*, April 2009.

[9] S. Traverso, M. Ariaudo, I. Fijalkow, J-L Gautier, and C. Lereau, "Decision Directed Channel Estimation and High I/Q Imbalance Compensation in OFDM Receivers," *IEEE Transactions on Communications*, Feb. 2008.

[10] P.F. Morlat, X. Gallon, and G. Villemaud, "Measured Performances of a SIMO Multi-Standard Receiver," *European Conference on Antennas and Propagation EUCAP07, Edinburgh*, November 2007.

[11] J.G. Proakis, *Digital communications*, Mc Graw Hill internationnal editions, 3rd edition, 1995.

[12] R. Kohno, R. Meidan, and L.B. Milstein, "Spread spectrum access methods for wireless communications," *IEEE Communications Magazine*, vol. 33, no. 1, pp. 58–67, Janvier 1995.

[13] "Wireless MAN Medium Access Control and Physical Specification," *IEEE Std 802.11*, 1999.

[14] www.agilent.com, ," .

[15] H. Schulze and C. Lueders, *Theory and Applications of OFDM and CDMA: Wideband Wireless Communications*, Wiley, 2005.